

PROF. SHING-TUNG YAU'S CONTRIBUTIONS TO APPLIED MATHEMATICS AND ENGINEERING

XIANFENG GU

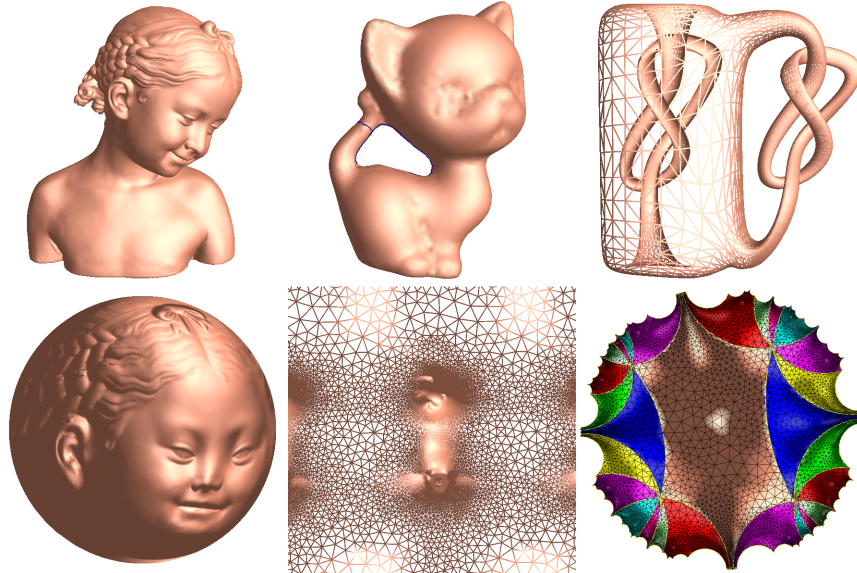


FIGURE 1. Surface uniformization.

Prof. Shing-Tung Yau is one of the greatest mathematicians in the human history. He has made tremendous contributions to fundamental sciences, especially mathematics and physics. He is the father of geometric analysis, which combines geometry with analysis. In applied mathematics field, he is also the father of computational conformal geometry, which combines geometry with computer science, and applies for many engineering and medical fields. Recently, Prof. Yau also developed theories and algorithms for optimal transportation, which lays down the foundation for artificial intelligence. This work will briefly summarize Prof. Yau's contributions in applied mathematics and engineering fields.

1. COMPUTATIONAL CONFORMAL GEOMETRY

Conformal geometry has deep roots in pure mathematics fields, such as Riemann surface theory, complex analysis, differential geometry, algebraic topology, partial differential equations and others. Historically, conformal geometry has been broadly

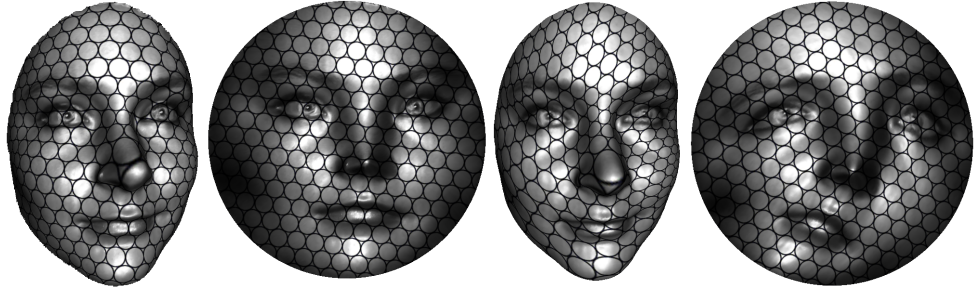


FIGURE 2. Left two frames: conformal mapping transforms infinitesimal circles to infinitesimal circles; Right two frames: general diffeomorphism maps infinitesimal ellipses to infinitesimal circles.

used in many engineering applications [1], such as electro-magnetics, vibrating membranes, acoustics, elasticity, heat transfer and fluid flow. Most of these applications depend on conformal mappings between planar domains. Recently, with the rapid development of 3D scanning and medical imaging technologies, 3D geometric data has become ubiquitous. It is challenging to process the huge amount of this geometric data with high accuracy and efficiency. The challenge can be tackled using various geometric theories.

Prof. Yau lead his students and collaborators to create a novel field “Computational Conformal Geometry”. Compared to topology or Riemannian geometry, conformal geometry better fits this purpose because conformal structure has much richer information than topological structure and conformal mappings are much more flexible than isometries. With the increase of computational power and further advances in mathematical theories, computational conformal geometry emerges as an interdisciplinary field, bridging mathematics and computer science. Computational conformal geometric theories and algorithms have been generalized from planar domains to surfaces with arbitrary topologies and have been applied to many engineering and medical fields.

1.1. Basic Concepts. Suppose $\varphi : (S, \mathbf{g}) \rightarrow (D, \mathbf{h})$ is a diffeomorphism, such that the pull back metric and the original metric differ by a scalar function, $\varphi^*\mathbf{h} = e^{2u}\mathbf{g}$, then φ is called a *conformal mapping*. Conformal maps can also be characterized as those smooth maps which preserve infinitesimal circles. In Fig. 2, two diffeomorphisms map a female facial surface to the planar unit disk. The left two frames show a conformal mapping, which infinitesimally maps circles on the face to the infinitesimal circles on the disk. In contrast, the right frames illustrate a general diffeomorphism which maps infinitesimally ellipses to circles and not vice versa. If the eccentricities of the ellipses (the ratio between the major axis and the minor axis) are uniformly bounded, then the mapping is called a *quasi-conformal map*.

The *uniformization theorem* of Poincaré and Koebe proved states that every simply connected Riemann surface is conformally diffeomorphic to the 2-sphere \mathbb{S}^2 , the plane \mathbb{E}^2 or the open unit disc \mathbb{H}^2 , as shown in Fig. 1. Using covering space theory, the uniformization theorem implies that every connected oriented surface with a Riemannian metric (S, g) is conformally diffeomorphic to one of three canonical models of surfaces: (i) the unit sphere \mathbb{S}^2 , (ii) a flat torus \mathbb{E}^2/Γ , or \mathbb{E}^2 , or $\mathbb{E}^2 - \{0\}$ or (iii) a hyperbolic surface \mathbb{H}^2/Γ where Γ is a discrete torsion free subgroup of isometries of the hyperbolic plane \mathbb{H}^2 . The uniformization theorem also holds for compact surfaces with boundaries. As shown in Fig. 3, Riemannian metric surfaces with boundaries can be conformally mapped to the canonical surfaces with constant curvatures with a finite number of geodesic disks removed.

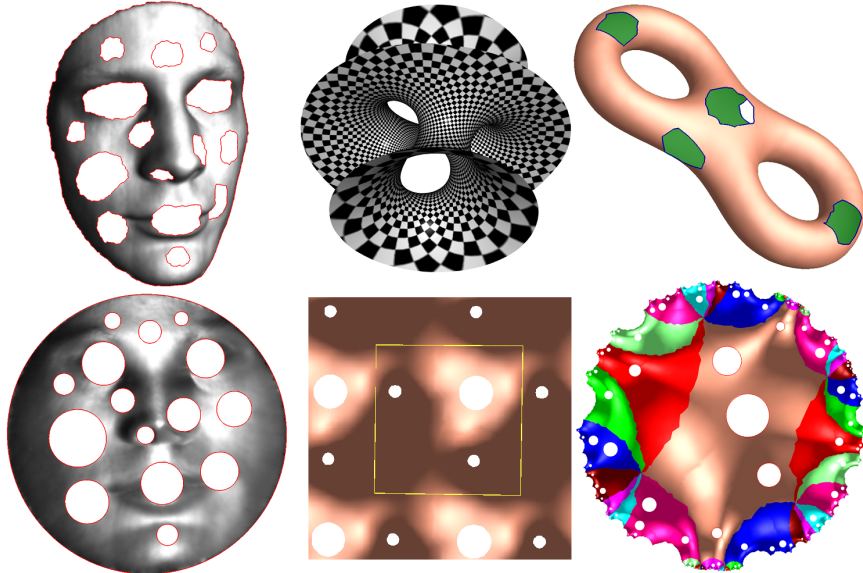


FIGURE 3. Uniformization for surfaces with boundaries.

The uniformization theorem plays a fundamental role for applications in engineering and medical imaging. It sorts all kinds of shapes in the real physical world to only three canonical types. If one can develop an algorithm that can handle the canonical type surfaces, then the algorithm can process all shapes via uniformization. This greatly simplifies the algorithmic design task for engineers.

1.2. Computational Methods. With the advances of modern technologies, surfaces are produced digitally at an alarming rate these days. There is an urgent need to process and categorize them. A useful form of these digital surfaces is polyhedral surfaces. Prof.Yau developed theories and computational algorithms to discretize smooth surface with high accuracy in [2]. In Fig. 4 Michelangelo's David sculpture surface is approximated by a polyhedral surface. Classical differential geometric

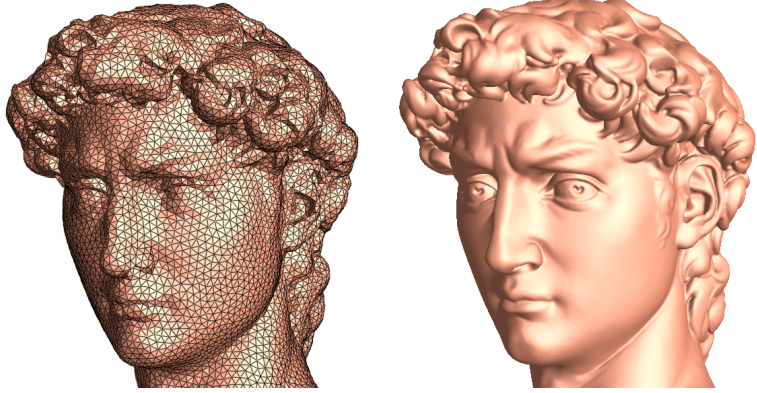


FIGURE 4. Discrete representation of Michelangelo’s David sculpture surface.

theories are inadequate to deal with polyhedral and digital surfaces. It is a major challenge to develop computable theories for conformal, harmonic, quasiconformal, isometric, area preserving and other mappings for polyhedral surfaces. There are several guiding principles one tries to follow in discretizing classical concepts. Firstly, the discrete counterparts should have their own intrinsic geometric structures. Secondly, there should be a finite dimensional variational principle whose critical points would correspond to the discrete entities. As usual, a finite dimensional variational characterization will then lead to practical computational algorithms with efficiency, accuracy and robustness. Finally, the discrete entities should converge to their smooth counterparts when the triangular meshes are suitably chosen.

There are three categories of computational algorithms [3, 10, 11], as illustrated in the computation of surface uniformization Fig. 1: harmonic maps method in the left frame, Hodge decomposition and meromorphic differential method in the middle frame and the discrete surface Ricci/Yamabe flow method in the right frame. Different methods have different advantages and disadvantages, and are able to solve different problems. None of them can be replaced by others. For example, in order to find the conformal hyperbolic metric, discrete curvature flow should be used; in order to compute holomorphic differentials, Hodge decomposition method should be applied and so on.

1.2.1. Harmonic Maps. Prof.Yau generalized harmonic maps method from Riemannian manifolds to the discrete setting and introduced he spherical harmonic map algorithm [6, 34], which computes harmonic maps for genus zero closed surfaces. Intuitively, the harmonic energy measures the elastic deformation energy (harmonic energy) induced by a mapping between surfaces. It depends on the Riemannian metric of the target surface and the conformal structure of the source surface. Harmonic maps are the critical points of the harmonic energy within the homotopy class. If



FIGURE 5. A spherical harmonic mapping from the Stanford bunny surface (left frame) onto the unit sphere (middle frame), and to an area preserving map using spherical optimal transportation (right frame).

the target surface has negative Gaussian curvature, and the mapping degree is one, then the harmonic mapping is diffeomorphic [26]. A mapping between two surfaces induces the so-called Hopf differential on the source surface. If the mapping is harmonic, then its Hopf differential is a holomorphic quadratic differential on the source surface. Furthermore, if the Hopf differential is zero, then the mapping is conformal. Since holomorphic quadratic differentials on a genus zero surface must be zero, harmonic maps between genus zero closed surfaces must be conformal. Therefore, this method can also produce conformal mappings between genus zero surfaces.

In practice, the algorithm first constructs the Gauss map from the input surface to the unit sphere, then uses the non-linear heat diffusion method to reduce the harmonic energy to reach a harmonic map. More specifically, the method computes the Laplacian of the map, update the image of each point along the tangential direction of the Laplacian. Different harmonic maps differ by a Möbius transformation of the unit sphere, therefore the algorithm adds an extra normalization constraint to ensure the uniqueness of the mapping. During the heat diffusion, the algorithm ensures that the mass center of the image of the surface on the unit sphere stays at the origin. The efficiency of the algorithm depends on the initial mapping. One way to further improve the efficiency is to divide the surface into two segments along the Nordahl curve of the first eigen function of the Laplace-Beltrami operator and then embed each segment onto the unit disk with consistent Dirichlet boundary condition using (linear) harmonic maps.

1.2.2. Hodge Decomposition. Prof. Yau and his student introduced the algorithm based on Hodge decomposition theorem in [8, 12], the so-called Gu-Yau algorithm. Hodge decomposition says that any differential form ω on a closed Riemannian manifold can be uniquely written as the sum of three parts: $\omega = d\alpha + \delta\beta + \gamma$, where γ is harmonic, that is $\Delta\gamma = 0$ with $\Delta = d\delta + \delta d$. Intuitively, this can be interpreted as follows: Any



FIGURE 6. Two conjugate harmonic one-forms, in the left and middle frames, combine to form a holomorphic one-form in the right frame. The loops in the left (middle) frame show the vertical (horizontal) trajectories of the holomorphic form.

vector field on a surface can be decomposed into three components: a curl-free part, divergence-free part and harmonic part. A vector field is harmonic if and only if it has zero curl and zero divergence, as shown in Fig. 6.

The Gu-Yau algorithm first computes the homology group basis of the surface $H_1(S, \mathbb{Z})$, then the cohomology group basis of $H^1(S, \mathbb{R})$. For each closed one-form ω representing a basis in $H^1(S, \mathbb{R})$, the algorithm finds a function $f : S \rightarrow \mathbb{R}$, such that $\delta(\omega + df)$ is zero. This is a linear elliptic geometric partial differential equation, and can be solved using the Finite Element Method generalized to the Riemannian surface setting. Then $\omega + df$ is a harmonic one-form. Finally, the harmonic one-form paired with its conjugate form a holomorphic one-form. As shown in Fig. 6, the left frame shows a harmonic one-form ω , the middle frame shows the conjugate harmonic one-form ${}^*\omega$, and the right frame shows a holomorphic one-form $\omega + \sqrt{-1}{}^*\omega$. Using this method, the method can construct the basis of the group of holomorphic one-forms of the Riemann surface. By linear combination, the algorithm can then construct any holomorphic one-form.

Suppose S is a topological annulus with a Riemannian metric \mathbf{g} and the boundary of S are two loops $\partial S = \gamma_1 - \gamma_2$. The algorithm compute a holomorphic one-form ω , such that the imaginary component of the integration of ω along γ_1 is 2π . Upon fixing a point q , the conformal mapping $\varphi(p) = \exp(\int_q^p \omega)$ maps the surface onto a canonical annulus, as shown in Fig. 7.

Suppose S is a surface of genus zero with multiple boundaries, $\partial S = \gamma_0 - \gamma_1 - \gamma_2 - \dots - \gamma_n$, then S is called a multiply connected annulus. The algorithm can construct a unique holomorphic one-form ω , such that the imaginary part of the integration of ω along γ_0 is 2π , -2π along γ_1 , and 0 along other boundary components. Then, upon fixing a base point q , the conformal mapping $\varphi(p) = \exp(\int_q^p \omega)$ maps the surface onto

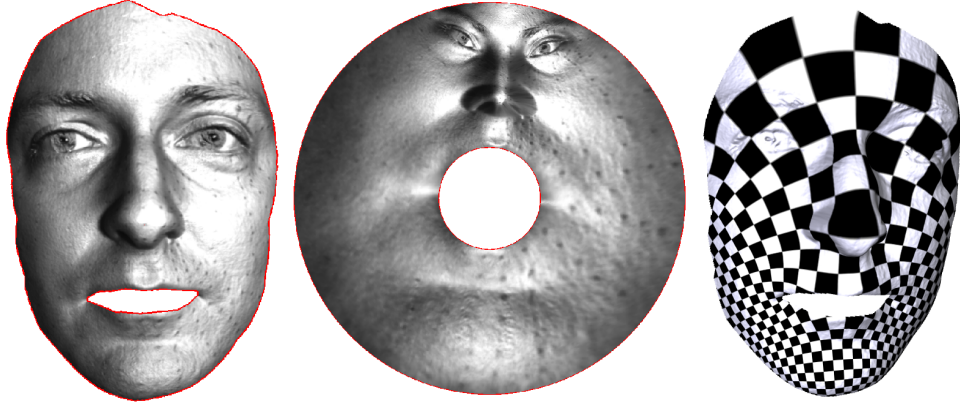


FIGURE 7. Topological annulus.

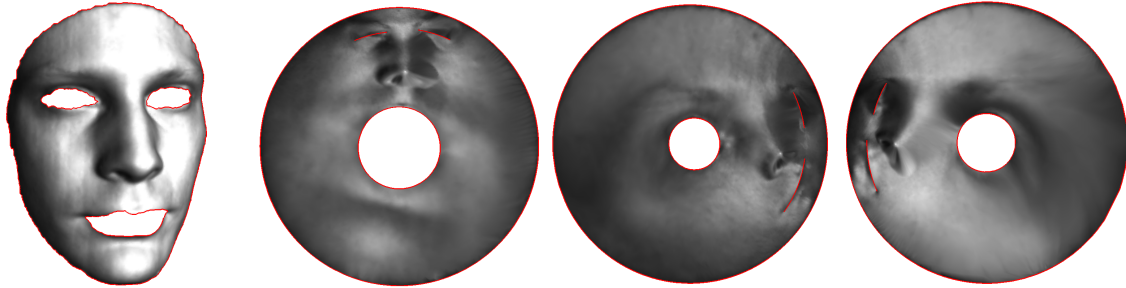


FIGURE 8. Circular slit mapping.

a canonical annulus with concentric circular slits, as shown in Fig. 8. The algorithm was introduced in [36].

Fig. 9 demonstrates Koebe's iteration algorithm [14], that conformally maps a multiply connected annulus onto a circle domain, namely the complement of the union of a finite number of disks. On the top row, we fill all the inner holes of the surface except one, then conformally map the topological annulus onto a canonical annulus; in the middle row, we fill the center circular hole and open another hole, map the topological annulus onto a canonical annulus; at the bottom row, we fill the center circular hole and open the 3rd hole, and map the topological annulus onto a canonical annulus. We repeat this procedure, opening different holes in order and filling other holes, then map the topological annulus to the canonical annulus. The boundaries become rounder and rounder, and the image converges to a circle domain exponentially fast. The method combined with conformal welding can be applied for shape analysis [23, 38]. An alternative method is given in [24], which is based on variational approach and complex analysis.

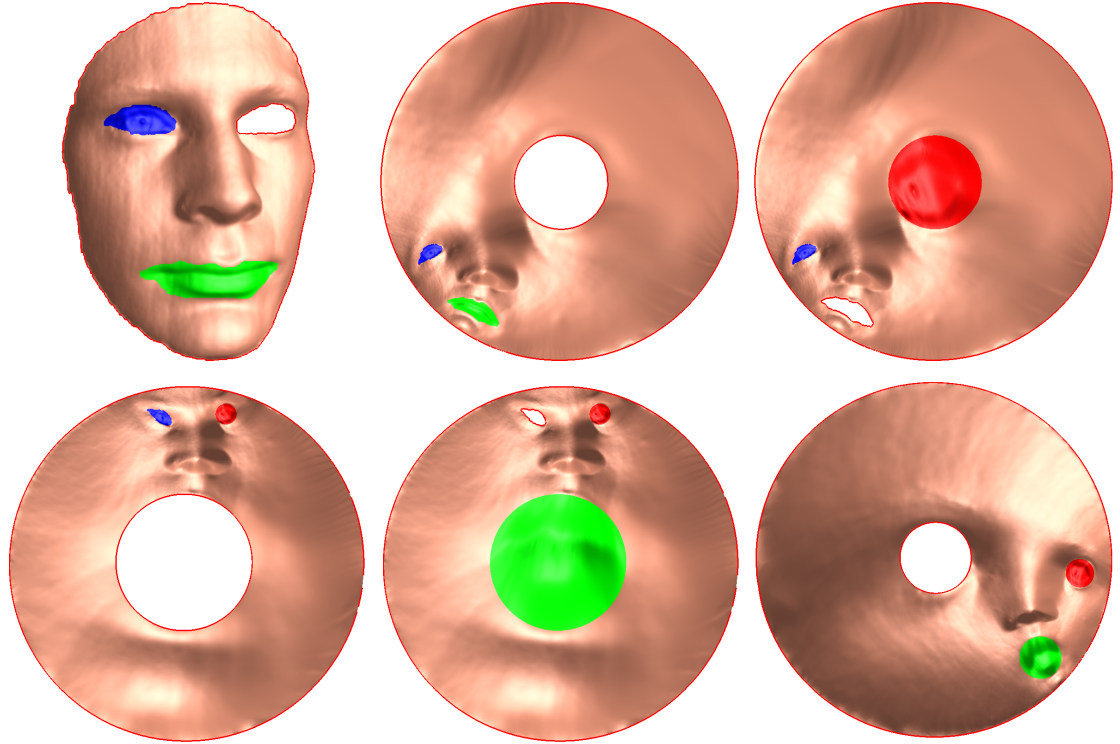


FIGURE 9. Koebe's iteration algorithm.

1.2.3. *Discrete Ricci Flow.* Prof.Yau, his students and collaborators have systematically generalized Ricci flow theory to the discrete setting [33, 40]. Ricci flow deforms the Riemannian metric proportional to the curvature, such that the curvature evolves according to a non-linear heat-diffusion process, and eventually becomes constant everywhere.

In discrete setting, surfaces are represented as simplicial complexes (S, \mathcal{T}) with polyhedral metrics. The Riemannian metric is represented as edge lengths $l : E(\mathcal{T}) \rightarrow \mathbb{R}_{>0}$ satisfying triangle inequalities. The discrete Gaussian curvature is defined as the angle deficit $K : V(\mathcal{T}) \rightarrow \mathbb{R}$,

$$K(v_i) = 2\pi - \sum_{jk} \theta_i^{jk},$$

where θ_i^{jk} is the corner angle at v_i in the face $[v_i, v_j, v_k]$. The total curvature satisfies the Gauss-Bonnet theorem,

$$\sum_v K(v) = 2\pi\chi(S),$$

where $\chi(S)$ is the Euler characteristic number of S . There are many ways to define conformal metric deformation, such as tangential circle packing, Thurston's circle



FIGURE 10. The extremal length of a topological quadrilateral.

packing, inversive distance circle packing, discrete Yamabe flow and virtual radius circle packing. All these schemes have been unified in Yau's work [40]. In Yamabe flow scheme, the algorithm defines discrete conformal factor as a function $u : V(\mathcal{T}) \rightarrow \mathbb{R}$, and the vertex scaling as

$$l_{ij} \leftarrow e^{u_i} l_{ij} e^{u_j}.$$

Two polyhedral metrics \mathbf{d}, \mathbf{d}' on a punctured surface (S, V) are conformally equivalently, if there exists a sequence of PL metrics with the corresponding triangulations

$$(\mathbf{d}_0, \mathcal{T}_0), (\mathbf{d}_1, \mathcal{T}_1) \cdots, (\mathbf{d}_n, \mathcal{T}_n),$$

where $\mathbf{d}_0 = \mathbf{d}$ and $\mathbf{d}_n = \mathbf{d}'$, such that \mathcal{T}_k is Delaunay with respect to \mathbf{d}_k ; if \mathcal{T}_i and \mathcal{T}_{i+1} are identical, then \mathbf{d}_i and \mathbf{d}_{i+1} differ by a vertex scaling; if \mathcal{T}_i and \mathcal{T}_{i+1} differ by an edge swap, then \mathbf{d}_i and \mathbf{d}_{i+1} are isometric.

Given any target curvature $\bar{K} : V(\mathcal{T}) \rightarrow (-\infty, 2\pi)$, satisfying the Gauss-Bonnet condition, then there exists a unique metric \mathbf{d}' , which is discrete conformal to the initial metric \mathbf{d} , \mathbf{d}' induces the target curvature \bar{K} . The metric can be obtained by the discrete Ricci flow

$$\frac{du(v_i)}{dt} = \bar{K}(v_i) - K(v_i),$$

which is the gradient flow of the discrete entropy energy

$$E(\mathbf{u}) = \int^{(u_1, u_2, \dots, u_n)} \sum_{v_i \in V(\mathcal{T})} (\bar{K}(v_i) - K(v_i)) du(v_i).$$

The convexity of the entropy energy ensures the uniqueness of the solution. The variational problem can be solved using Newton's method.

It is proved in [5] that if \mathbf{g} is a Riemannian metric on a compact manifold M and $u : M \rightarrow \mathbb{R}$ is a smooth function, then there exists a constant $C > 0$ such that for any pairs of points $x, y \in M$, $|d_{e^{4u}\mathbf{g}}(x, y) - e^{u(x)+u(y)} d_{\mathbf{g}}(x, y)| \leq C d_{\mathbf{g}}(x, y)^3$. Here $d_{\mathbf{g}}$ is the Riemannian distance associated to the Riemannian metric \mathbf{g} , i.e., $d_{\mathbf{g}}(x, y)$ is the infimum of the lengths of all paths joining x to y . The above estimate holds the key for showing that discrete conformal maps defined using (??) converge to the smooth case.

Fig. 10 shows one example of computing the extremal length of a topological quadrilateral using discrete Ricci flow. Basically, we set the target curvature to be zero for all interior and boundary vertices, except the four corners, and set the target curvatures for the corners to be $\pi/2$. Then we run Ricci flow to get the target metric, and isometrically embed the surface using the target metric to obtain the planar rectangle. Here the discrete curvature at a boundary vertex is defined to be π less the sum of all angles at v .

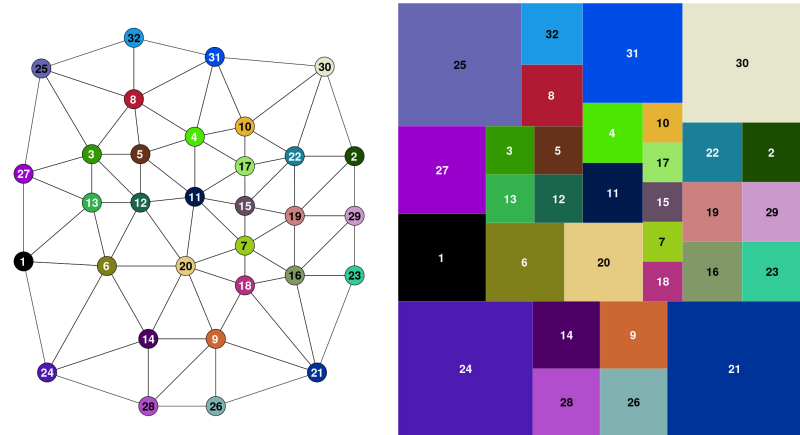


FIGURE 11. Square tiling of a 3-connected graph, each node is replaced by a square with the same label and color. Two nodes are connected in the graph, if and only if their corresponding squares are tangent.

Fig. 11 shows a generalization of circle packing by replacing circles by squares to compute the extremal length of a combinatorial quadrilateral. The left frame shows a 3-connected graph, with four corner nodes. The right frame shows the extremal length, where each node is replaced by a square with the same label and color. Two nodes are connected in the graph if and only if their corresponding squares are tangent. In theory, squares can be replaced by more general convex shapes.

The method can be generalized to surfaces with hyperbolic background geometry. Fig. 12 shows an example for computing the hyperbolic metric on a high genus surface. As shown in the left frame, the input surface is triangulated, and each face is a hyperbolic triangle instead of a Euclidean triangle. The theoretic formulation and the algorithmic details are very similar. After obtaining the uniformization metric, we isometrically embed a finite portion of the universal covering space of the surface onto the Poincaré model of \mathbb{H}^2 . Each color represents a fundamental polygon, and the boundaries of the fundamental polygons are hyperbolic geodesics. The hyperbolic Ricci flow is applied for shortest word problem in computational topology in [37], and computing the Fenchel-Nielsen coordinates in Teichmüller shape space in [13].

2. QUASI-CONFORMAL MAPPING

Prof. Yau and collaborators have also generalized the theories and algorithms for conformal mappings to quasi-conformal mappings [18–21, 35, 39]. If two compact surfaces are with different conformal moduli, there is no conformal mappings between them. All the diffeomorphisms between them are *quasi-conformal mappings*.

A conformal mapping transforms infinitesimal circles to infinitesimal circles, a quasi-conformal mappings transforms them to infinitesimal ellipses. The eccentricities and orientations of the ellipses are encoded by the so-called Beltrami differentials.

Given a domain Ω on the complex plane, also given a measurable complex value function defined on the surface $\mu : \Omega \rightarrow \mathbb{C}$, we want to find a quasi-conformal map $\phi : \Omega \rightarrow \mathbb{C}$, such that ϕ satisfies the Beltrami equation:

$$\frac{\partial \phi}{\partial \bar{z}} = \mu \frac{\partial \phi}{\partial z}.$$

The *auxiliary metric* method [35] constructs an auxillary Riemannian metric $|dz + \mu d\bar{z}|^2$, such that the quasi-conformal map $\varphi : (\Omega, |dz|^2) \rightarrow (\mathbb{D}, |dw|^2)$ is quasi-conformal, the exact same mapping $\varphi : (\Omega, |dz + \mu d\bar{z}|^2) \rightarrow (\mathbb{D}, |dw|^2)$ becomes conformal. Hence it can be obtained by using the conformal mapping algorithms. Figure ?? illustrates quasi-conformal mappings for a human facial surface.

In each homotopy class of the measurable mappings between two surfaces, there is a Teichmüller map φ^* which minimizes the L^∞ of the Beltrami coefficient μ_φ . As shown in Fig. 13, for a Teichmüller map, all the infinitesimal ellipses have the same eccentricity, namely the norm of μ is constant. The Teichmüller map can be carried out by an iterative method introduced in [18]: first, μ_0 is set to be zeros, then the

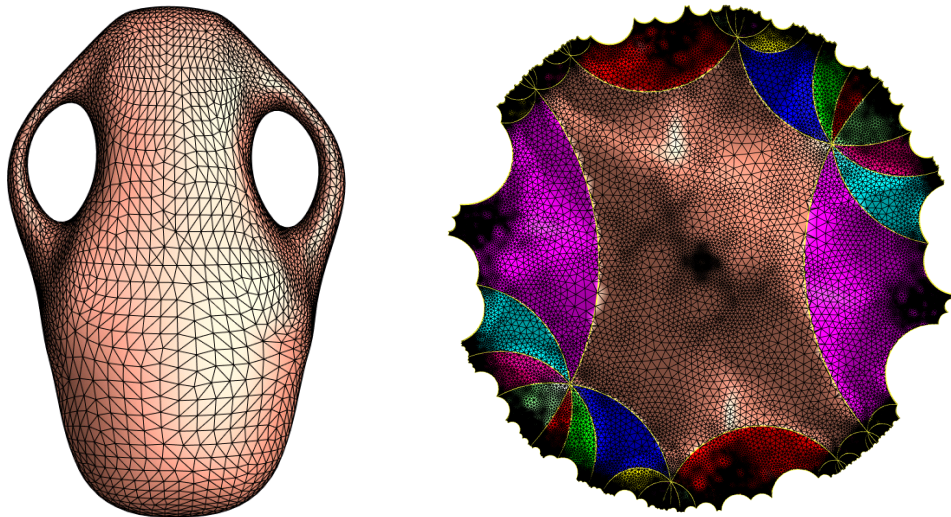


FIGURE 12. Uniformization for high genus surfaces.

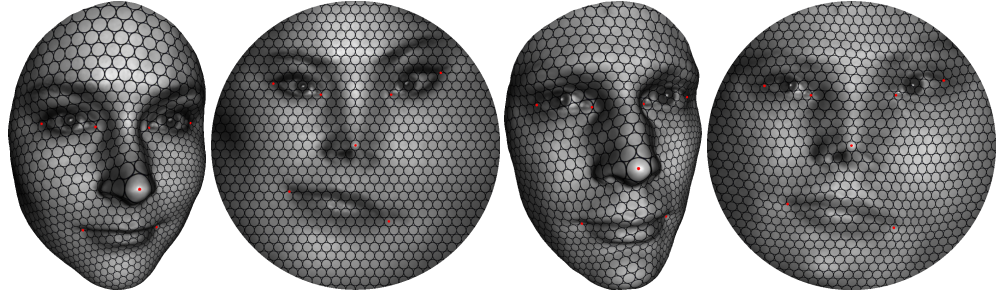


FIGURE 13. Teichmüller map.

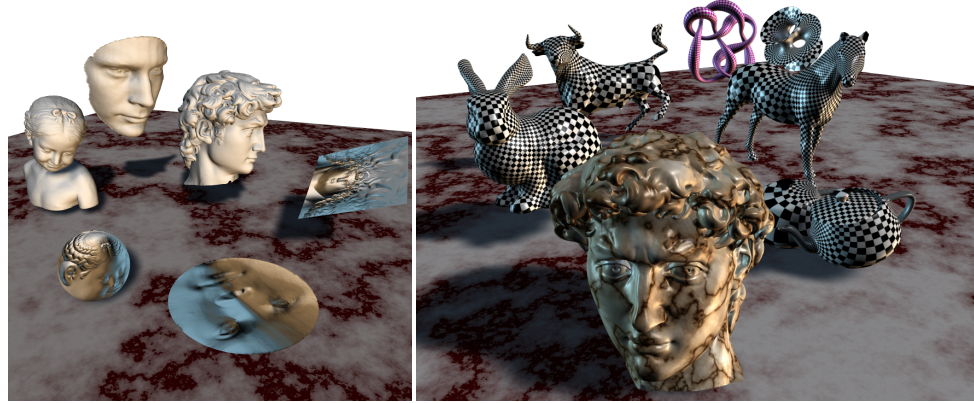


FIGURE 14. Global conformal surface parameterization for texture mapping.

algorithm computes the harmonic map $\varphi_k : (\Omega, \mu_k) \rightarrow \mathbb{D}$, then set

$$\mu_{k+1} \leftarrow c \frac{\mu_{\varphi_k}}{|\mu_{\varphi_k}|}, \quad c \leftarrow \frac{1}{2i|\Omega|} \int_{\Omega} |\mu_{\varphi_k}| dz \wedge d\bar{z}.$$

The mappings $\{\varphi_k\}$ converge to the Teichmüller map. Fig. 13 shows the Teichmüller map between two human facial surfaces with landmark constraints [19]. It is easy to see that all the ellipses are with the same eccentricity.

2.1. Applications. Computational conformal geometry has been broadly applied in many engineering fields. In the following, we briefly introduce some of our recent projects, which are the most direct applications of computational conformal geometry in the computer science field.

2.1.1. Computer Graphics. Conformal geometric methods have broad applications in computer graphics [8, 12, 28]. In computer-generated movies and games, shapes are modeled as triangular polyhedral surfaces, and the skins and clothes are represented as planar images, which are called texture images. *Surface parameterization* technique refers to the process of mapping a surface onto a planar domain. Once the surfaces

are parameterized onto planar domains, the texture images are pulled back onto the surface to achieve a photorealistic visual effect, and this technique is called *texture mapping*. Texture mapping is one of the most fundamental techniques in the computer graphics field. Isothermal coordinates are natural for global surface parameterization purposes. Because conformal mapping doesn't distort the local shapes, it is desirable for texture mapping. Fig. 14 shows an example of texture mapping constructed using holomorphic differentials.



FIGURE 15. 3D human facial surface data scanned using structured light technology.

2.1.2. Computer Vision. Prof.Yau developed a 3D scanning system, which is capable of capturing dynamic 3D surfaces with high accuracy and high speed [9]. The method is based on multi-wavelength phase shifting and uses Chinese Remainder theorem for phase unwrapping algorithm.

Surface matching is a fundamental problem in computer vision, which aims at finding a diffeomorphism between two surfaces with landmark constraints and least distortion. Fig. 16 illustrates one example of matching of two human facial surfaces. The surfaces are conformally mapped onto the planar unit disks by Riemann mappings. The major feature points are located based on the geometry and the texture information using either a geometric method or statistical learning method, which are shown as red dots. The problem of finding a diffeomorphism between facial surfaces is converted to finding one between the planar disks, and the latter one is much simpler and more efficient to compute.

The quasi-conformal mapping algorithm based on *auxiliary metric method*. [35] are applied for surface matching. The Teichmüller mapping algorithms [18, 18, 19, 39] are applied for surface matching directly, which can guarantee the mappings are diffeomorphisms with least angle distortion, furthermore the existence and the uniqueness of the solutions are also ensured by the Teichmüller theory. Harmonic

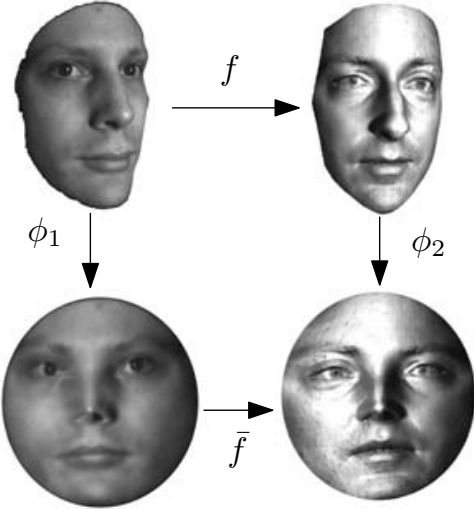


FIGURE 16. Surface matching framework.

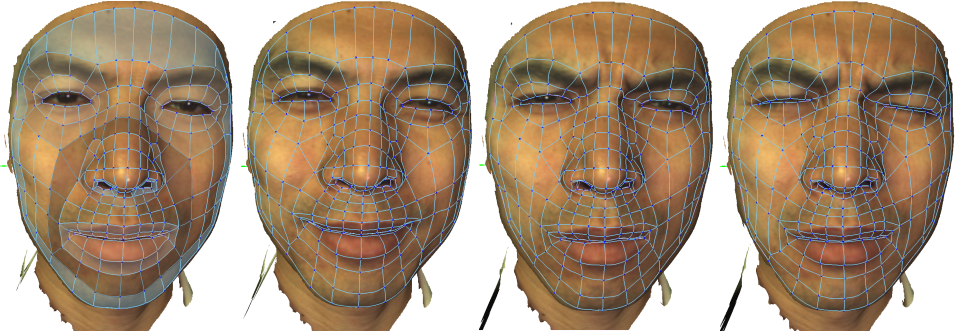


FIGURE 17. Facial expression tracking.

maps between surfaces with hyperbolic metrics are also diffeomorphic and are unique with each homotopy class. Therefore, hyperbolic harmonic map method is also applied for surface registration as introduced in [26].

Given a sequence of facial surfaces with dynamic expression change, the Teichmüller map can be used to find natural diffeomorphisms among them. The trajectories of the feature points give the facial expression, which can be transferred to other models for animation purposes. Fig. 17 demonstrates an expression tracking result; the blue quadrilateral mesh is attached to the facial surface and moves along with it. The trajectories of the vertices of the blue mesh represent the expression.

There are more applications of conformal geometry in computer vision. Surfaces can be classified by conformal equivalence by computing period matrices [7]. Conformal welding and conformal structure are applied for defining planar shape space in [22].

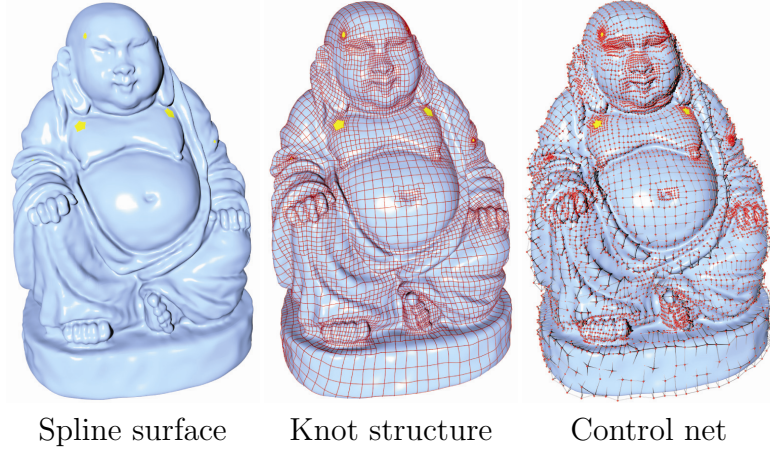


FIGURE 18. A spline surface with prescribed singularities (the centers of the yellow regions). The *control net* controls the shape, the *knot structure* describes the local chart of the atlas.

2.1.3. Geometric Modeling. In the conventional manufacturing industry, the representation of shapes needs to have higher-order continuity. The embedding of triangular meshes is only continuous but not differentiable. Therefore, the meshes need to be converted to piecewise polynomial representations with C^2 continuity almost everywhere, such as NURBS or T-Splines. It has fundamental importance to convert polyhedral surfaces to Splines.

Prof. Yau and his colleagues showed that classical Splines are based on affine geometric invariants, therefore if a surface admits an affine structure then it can be converted to a global Spline surface. Unfortunately, due to topological obstructions, general closed surfaces do not admit any affine structure. It is proven in [4] that one can minimizes the number of singularities of the Spline surface to one. As shown in Fig.18, the left frame shows the Spline surface of a Buddha model, the middle frame shows the knot structure and the right frame the control net. The yellow spots shows the singularities, where the Spline surface is only C^1 continuous.

2.1.4. Medical Imaging. Conformal geometry has been applied to many fields in medical imaging. For example, in the field of brain imaging, it is crucial to register different brain cortex surfaces reconstructed from MRI or CT images. Because brain surfaces are highly convoluted, and different people have different anatomic structures, it is quite challenging to find proper matching between cortex surfaces. Cortex surfaces are topological spheres and can be uniformized onto the unit sphere conformally. Fig. 19 illustrates this solution [6, 33, 34] by mapping brains to the unit sphere in a canonical way. Then, by finding an automorphism of the sphere, the registration between cortical surfaces can be easily established.

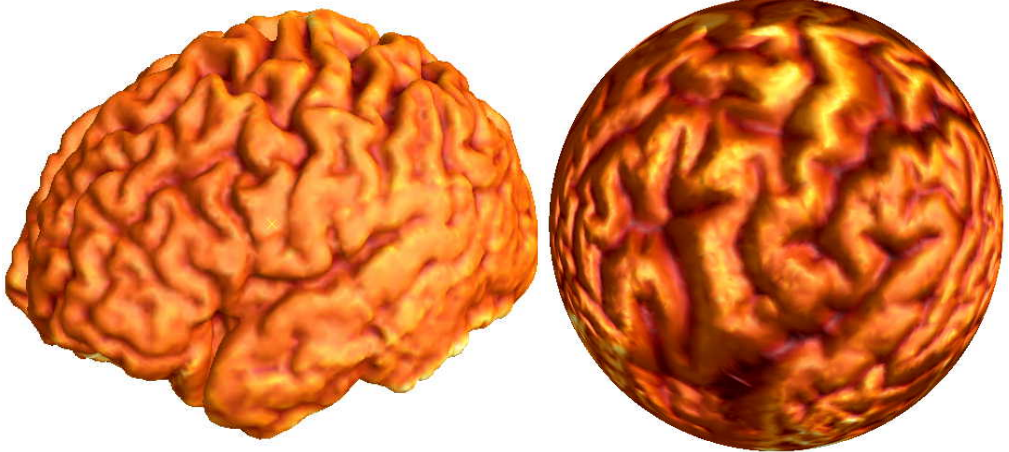


FIGURE 19. Brain spherical conformal mapping.

Another method is shown in Fig. 20. The major landmark curves (succi and gyri) on the cortical surfaces are located, then the surface is sliced open along these landmarks and conformally mapped onto a circle domain. The centers and radii of the inner circles give the conformal module of the surface, which can be treated as the fingerprint of the cortical surface and used for classification and comparison. These methods have been applied for neurological disease diagnosis, such as Alzheimer’s disease, autism, Williams syndrome, and so on. The cortical surface can be parameterized using slit map [31, 32]. Teichmüller space theory is applied from brain morphometry in [30] and [29], where the Teichmüller coordinates of the brain surface are obtained by hyperbolic Ricci flow. By using Ricci flow, one can assign a hyperbolic metric on the surface. Then cortical surfaces can be registered using hyperbolic harmonic maps [25, 27]. Quasi-conformal mapping method is applied for registering hippocampal shapes using Beltrami holomorphic flow in [17].

3. COMPUTATIONAL OPTIMAL TRANSPORT FOR ARTIFICIAL INTELLIGENCE

Recently, deep learning becomes the mainstream technique for machine learning tasks, including image recognition, machine translation, speech recognition and so on. Despite its success, the theoretic understanding of deep learning remains primitive. Prof.Yau, his students and collaborators have made fundamental contributions to explain the principles of deep learning by modern topology and geometry, especially the optimal transportation theory and Monge-Ampére equation.

Half of the human brain is devoted to vision, Helmholtz hypothesized that vision solves an inverse problem, i.e., inferring the most likely causes of the retina image. In modern language, the brain learns a generative model of visual images, and visual perception is to infer latent variables of this generative model. The generative model with its multiple layers of latent variables from a representation of our visual world.

About the representation learning, the basic idea is that the brain represents a concept by a group of neurons, or latent variables. Namely, a concept is embedded into a multi-dimensional latent space. In data science, this is formulated as a well-accepted *manifold distribution law*: a natural data class can be treated as a probability distribution defined on a low dimensional manifold embedded in a high dimensional ambient space. The manifold distribution law describes the intrinsic pattern for natural data class (a concept), therefore the central tasks of deep learning are to learn the manifold structure and learn the probability distribution. Optimal transport provides a solid theoretic foundation for learning the probability distribution.

3.1. Geometric Variational Method for Optimal Transport. Given two domains Ω and Ω^* with probability distributions μ and ν respectively, the density functions are given by $d\mu(x) = f(x)dx$ and $d\nu(y) = g(y)dy$, the total measures are equal $\mu(\Omega) = \nu(\Omega^*)$. A smooth mapping $T : \Omega \rightarrow \Omega^*$ is *measure-preserving*, if for Borel set $B \subset \Omega^*$, $\mu(T^{-1}(B)) = \nu(B)$, and denoted as $T_{\#}\mu = \nu$. The cost function $c : \Omega \times \Omega^* \rightarrow \mathbb{R}$, the transportation cost for T is defined as $\mathcal{C}(T) = \int_{\Omega} c(x, T(x))f(x)dx$. The Mongé's problem is to find the optimal transportation map:

$$\min_{T_{\#}\mu=\nu} \mathcal{C}(T) = \min_{T_{\#}\mu=\nu} \int_{\Omega} c(x, T(x))f(x)dx.$$

If the transportation cost is the L^2 Euclidean distance $c(x, y) = 1/2|x - y|^2$, Brenier's theorem claims that there exists a convex function $u : \Omega \rightarrow \mathbb{R}$, the so-called Brenier potential, such that the gradient of the Brenier potential gives the optimal transportation map $T = \nabla u$. By measure-preserving condition, the Brenier potential

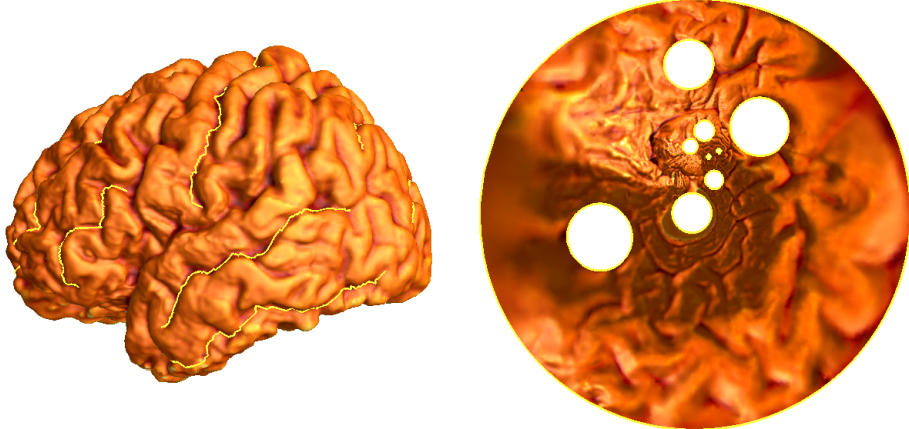


FIGURE 20. Brain morphology study using conformal module.

satisfies the Monge-Amperé equation:

$$\det \left(\frac{\partial^2 u(x)}{\partial x_i \partial x_j} \right) = \frac{f(x)}{g \circ \nabla u(x)}.$$

Therefore, Monge-Amperé equation plays a fundamental role in deep learning. Due to the highly non-linearity, it is challenging to solve the Monge-Amperé equation efficiently.

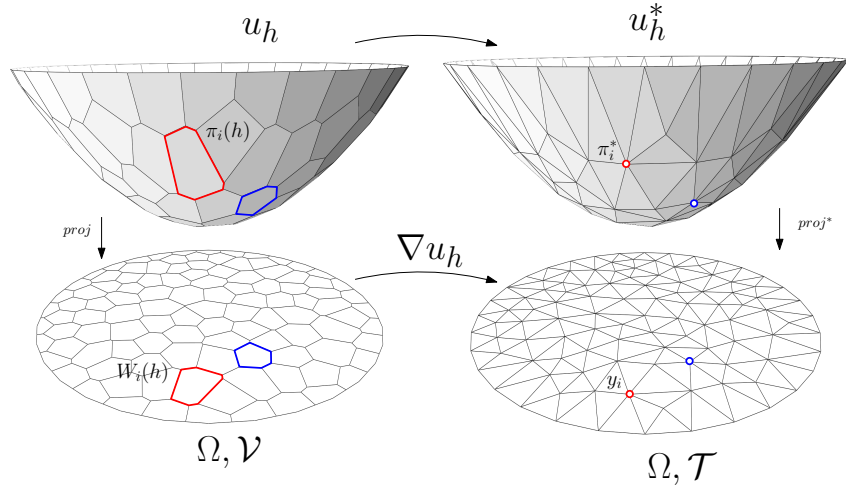


FIGURE 21. Discrete optimal transportation map.

Prof.Yau's team have discovered the intrinsic relation between Brenier's theory and Alexandrov's theory in convex geometry. Alexandrov's theorem states that : given a compact domain Ω in \mathbb{R}^n , p_1, p_2, \dots, p_k distinct points in \mathbb{R}^n , $A_1, A_2, \dots, A_k > 0$, such that $\sum A_i = \text{vol}(\Omega)$, there exists piecewise-linear convex function, the so-called Alexandrov potential,

$$u(x) = \max\{\langle x, p_i \rangle - h_i | i = 1, 2, \dots, k\}$$

unique up to vertical translation, such that

$$\text{vol}(W_i) = \text{vol}(\{x | \nabla u(x) = p_i\}) = A_i.$$

The Alexandrov potential is equivalent to the Brenier potential, unfortunately Alexandrov's existence proof is based on algebraic topological method and hard to convert to computational algorithm. Prof.Yau's team gave a constructive proof for Alexandrov's theorem based on variational principle in [5]. Yau's method reduces Alexandrov convex polytope construction to a optimize the following convex energy:

$$E(\mathbf{h}) = \sum_{i=1}^k A_i h_i - \int_0^{(h_1, h_2, \dots, h_k)} \sum_{i=1}^k w_i(\eta) d\eta,$$

where $w_i(\eta)$ is the μ -volume of the cell $W_i(\eta)$.

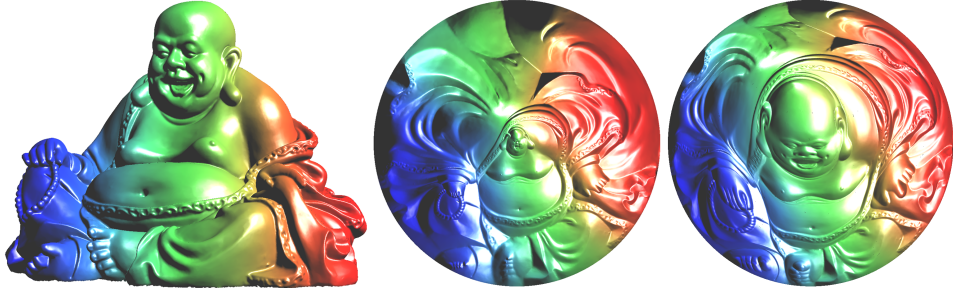


FIGURE 22. Semi-discrete optimal transportation map.

Fig. 22 shows an optimal transportation map computed using Yau's method. The buddha surface is conformally mapped onto the planar unit disk by a Riemann mapping $\varphi : (S, \mathbf{g}) \rightarrow (\mathbb{D}, |dz|^2)$, the metric \mathbf{g} can be represented as $\mathbf{g} = e^{2u}(dx^2 + dy^2)$. Then surface area element is pushed forwarded to the disk and induces a measure $\mu = e^{2u(x,y)}dx \wedge dy$. Fig. 22 shows the optimal transportation map from (\mathbb{D}, μ) to the uniform distribution on the unit disk. Fig. 23 shows the corresponding Brenier potential, and its Legendre dual.

3.2. Geometric Interpretation to Mode Collapsing. Conventional generative models in deep learning suffer from the so-called *mode collapsing* problem. The support of the target measure may have multiple connected components (modes). The learning process may only cover some of the modes and miss the others (mode collapsing), or cover all the modes but also the gaps among the modes (mode mixture). Furthermore, conventional models are sensitive to hyper-parameters and the training processes are highly unstable, difficult to converge. Prof. Yau's team discovered the intrinsic reason for mode collapsing using the regularity theory of Monge-Amperé equation [15, 16].

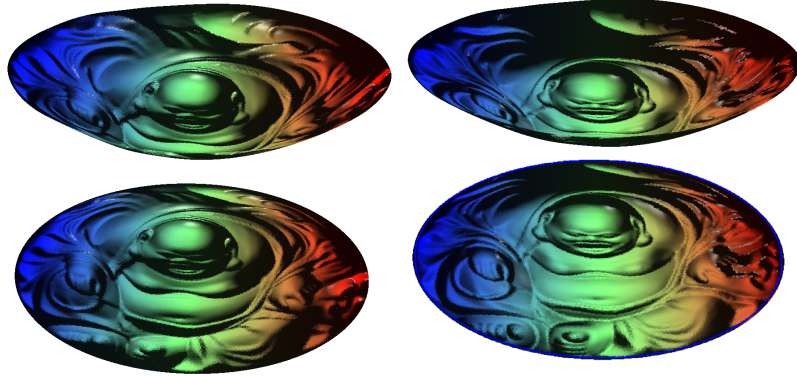


FIGURE 23. Brenier potential of the OT map.

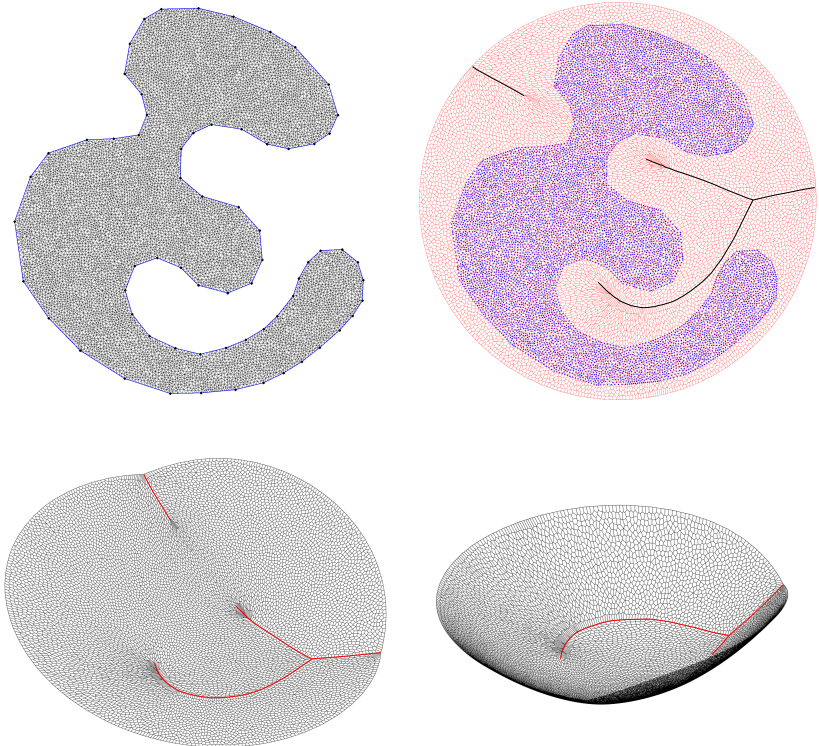


FIGURE 24. Singularity of optimal transportation map.

Conventional regularity theories of solutions to Monge-Amperé equation focus on convex target support cases. In deep learning, the support of the target measure may be concave. As shown in Fig. 24, then the Brenier potential is not C^1 globally. The locus of the projection of the non-differential points is the singularity, where the optimal transport map is discontinuous. Deep neural networks can only represent continuous mappings, but the transportation maps are discontinuous on singular sets. Namely, the target mappings are outside the functional space of Deep neural networks. This conflict induces mode collapsing. The optimal transport map is discontinuous, but Brenier potential itself is continuous. The neural network should represent the Brenier potential, instead of its gradient, namely the transportation map.

3.3. Generative Model Design. In order to eliminate mode collapsing, Prof. Yau's team developed novel generative model based on geometric theory of optimal transport in [1]. The model separate manifold learning and probability learning explicitly, and use geometric optimization method to solve Monge-Amperé equation for the optimal transportation map, this makes half of the black box of deep learning to be transparent.

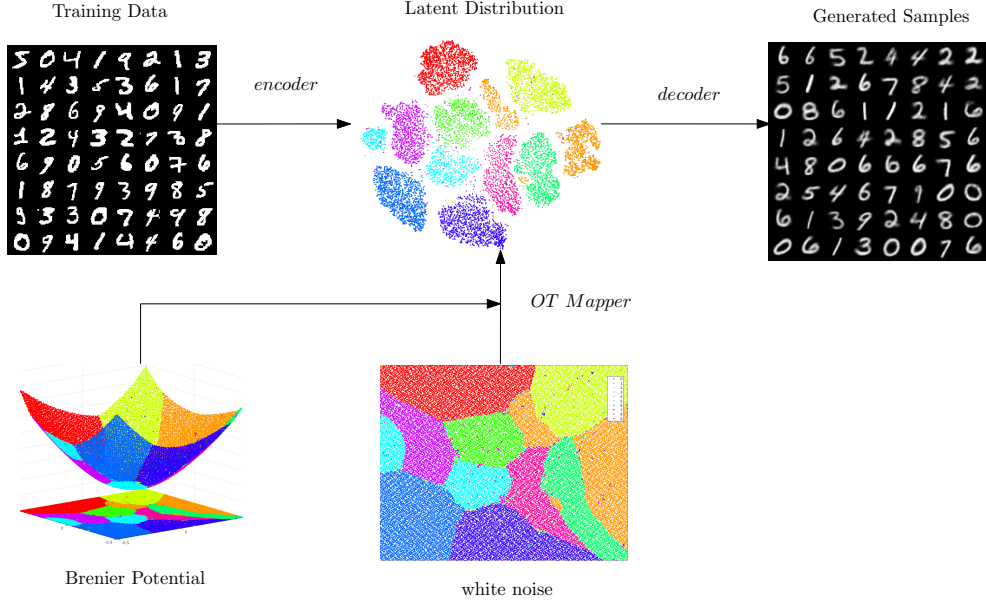


FIGURE 25. Generative model based on geometric optimal transportation.

Fig. 25 shows the geometric generative model, the encoder/decoder learn the manifold structure, the OT mapper maps the white noise to the latent data distribution. The optimal transport map is carried out by computing the Brenier potential based on the variational principle using Monte-Carlo method on GPUs. The MINST data set has ten modes, therefore the OT map is discontinuous at the singularity sets. The singularity set segments different clusters in the support of the white noise. The geometric generative model has many merits, it completely eliminates the mode collapsing, and mode mixture; solving Monge-Ampère equation is reduced to a convex optimization, which has unique solution. The optimization won't be trapped in a local optimum; The Hessian matrix of the energy has explicit formulation. The Newton's method can be applied with second order convergence; or the quasi-Newton's method can be used with super-linear convergence. Whereas conventional gradient descend method has linear convergence; The approximation accuracy can be fully controlled by the density of the sampling density by using Monte-Carlo method; The algorithm can be refined to be hierarchical and self-adaptive to further improve the efficiency; The parallel algorithm can be implemented using GPU.

Fig. 26 shows the realistic human facial images generated by the geometric generative model. This model is capable to find the boundary of the data manifold by locating the singularity set in the latent space. As shown in the right frame, a curve on the human facial image manifold is illustrated, each point represents a facial image. The curve starts from a boy image with brown eyes and ends at a girl with blue eyes. In the middle, there are images of human faces with one eye blue and one eye brown.



FIGURE 26. Human facial images generated by our geometric generative model.

Since the probability to encounter such kind of person is zero, therefore, those points are on the boundary of the support of the human facial image distribution. This demonstrates that the curve crosses the boundary of the manifold, which corresponds to the singularities of the optimal transportation map.

CONCLUSION

Prof. Yau has made fundamental contributions to applied mathematics and engineering, medical sciences. He has lead his students and colleagues to found interdisciplinary fields, including Computational Conformal Geometry and Computational Optimal Transportation. He has reshaped the minds of the whole generation of mathematicians, and greatly influenced the whole generation of engineers, researchers in various fields. History will prove his greatness, not only in pure mathematics, but also in many applied fields !

REFERENCES

- [1] Dongsheng An, Yang Guo, Na Lei, Zhongxuan Luo, Shing-Tung Yau, and Xianfeng Gu, *Ae-ot: A new generative model based on extended semi-discrete optimal transport*, Eighth international conference on learning representations (iclr), 2020.
- [2] Junfei Dai, Wei Luo, Miao Jin, Wei Zeng, Ying He, Shing-Tung Yau, and Xianfeng Gu, *Geometric accuracy analysis for discrete surface approximation*, Computer Aided Geometric Design **24** (2007), no. 6, 323–338.
- [3] David Xianfeng Gu, Feng Luo, and Shing-Tung Yau, *Fundamentals of computational conformal geometry*, Mathematics in Computer Science **4** (2010), no. 4, 389–429.
- [4] Xianfeng Gu, Ying He, Miao Jin, Feng Luo, Hong Qin, and Shing-Tung Yau, *Manifold splines with a single extraordinary point*, Computer-Aided Design **40** (2008), no. 6, 676–690.
- [5] Xianfeng Gu, Feng Luo, and Tianqi Wu, *Convergence of discrete conformal geometry and computation of uniformization maps*, Asian Journal of Mathematics (AJM) **23** (2019), no. 1, 21–34.

- [6] Xianfeng Gu, Yalin Wang, Tony F Chan, Paul M Thompson, and Shing-Tung Yau, *Genus zero surface conformal mapping and its application to brain surface mapping*, IEEE Transaction on Medical Imaging (TMI) **23** (2004), no. 8, 949–958.
- [7] Xianfeng Gu and S-T Yau, *Surface classification using conformal structures*, Ninth ieee international conference on computer vision, 2003. proceedings., 2003, pp. 701–708.
- [8] Xianfeng Gu and Shing-Tung Yau, *Global conformal surface parameterization*, Proceedings of the 2003 eurographics/acm siggraph symposium on geometry processing, 2003, pp. 127–137.
- [9] Xianfeng Gu, Song Zhang, Peisen Huang, Liangjun Zhang, Shing-Tung Yau, and Ralph Martin, *Holoiimages*, Proceedings of the 2006 acm symposium on solid and physical modeling, 2006, pp. 129–138.
- [10] Xianfeng David Gu, Feng Luo, and S-T Yau, *Recent advances in computational conformal geometry*, Communication in Information and System **9** (2009), no. 2, 163–196.
- [11] Xianfeng David Gu, Wei Zeng, Feng Luo, and Shing-Tung Yau, *Numerical computation of surface conformal mappings*, Computational Methods and Function Theory **11** (2012), no. 2, 747–787.
- [12] Miao Jin, Yalin Wang, S-T Yau, and Xianfeng Gu, *Optimal global conformal surface parameterization*, Visualization, 2004. ieee, 2004, pp. 267–274.
- [13] Miao Jin, Wei Zeng, Ning Ding, and Xianfeng Gu, *Computing fenchel-nielsen coordinates in teichmuller shape space*, Communication in Information & Systems **9** (2009), no. 2, 213–234.
- [14] Everett Kropf, Xiaotian Yin, Shing-Tung Yau, and Xianfeng Gu, *Conformal parameterization for multiply-connected domains: Combining finite elements and complex analysis*, ACM Journal of Engineering with Computers **30** (2014), no. 4, 441–455.
- [15] Na Lei, Dongsheng An, Yang Guo, Kehua Su, Shixia Liu, Zhongxuan Luo, Shing-Tung Yau, and David Xianfeng Gu, *A geometric understanding of deep learning*, Journal of Engineering (2020).
- [16] Na Lei, Kehua Su, Li Cui, Shing-Tung Yau, and David Xianfeng Gu, *A geometric view of optimal transportation and generative model*, arXiv preprint arXiv:1710.05488 (2017).
- [17] LM Lui, TW Wong, XF Gu, PM Thompson, TF Chan, and ST Yau, *Hippocampal shape registration using beltrami holomorphic flow*, Medical image computing and computer assisted intervention (miccai), part ii, lncs, 2010, pp. 323–330.
- [18] Lok Ming Lui, Xianfeng Gu, and Shing-Tung Yau, *Convergence of an iterative algorithm for teichmüller maps via harmonic energy optimization*, Mathematics of Computation **84** (2015), no. 296, 2823–2842.
- [19] Lok Ming Lui, Ka Chun Lam, Shing-Tung Yau, and Xianfeng Gu, *Teichmuller mapping (t -map) and its applications to landmark matching registration*, SIAM Journal of Imaging Science **7** (2014), no. 1, 391–426.
- [20] Lok Ming Lui, Tsz Wai Wong, Wei Zeng, Xianfeng Gu, Paul M Thompson, Tony F Chan, and Shing Tung Yau, *Detection of shape deformities using yamabe flow and beltrami coefficients*, Inverse Problems and Imaging **4** (2010), no. 2, 311–333.
- [21] Lok Ming Lui, Tsz Wai Wong, Wei Zeng, Xianfeng Gu, Paul M Thompson, Tony F Chan, and Shing-Tung Yau, *Optimization of surface registrations using beltrami holomorphic flow*, Journal of scientific computing **50** (2012), no. 3, 557–585.
- [22] Lok Ming Lui, Wei Zeng, Shing-Tung Yau, and Xianfeng Gu, *Shape analysis of planar objects with arbitrary topologies using conformal geometry*, European conference on computer vision, 2010, pp. 672–686.
- [23] ———, *Shape analysis of planar multiply-connected objects using conformal welding*, IEEE transactions on pattern analysis and machine intelligence **36** (2014), no. 7, 1384–1401.

- [24] Wei Luo, Junfei Dai, Xianfeng Gu, and Shing-Tung Yau, *Numerical conformal mapping of multiply connected domains to regions with circular boundaries*, Journal of computational and applied mathematics **233** (2010), no. 11, 2940–2947.
- [25] Rui Shi, Wei Zeng, Zhengyu Su, Hanna Damasio, Zhonglin Lu, Yalin Wang, Shing-Tung Yau, and Xianfeng Gu, *Hyperbolic harmonic mapping for constrained brain surface registration*, Proceedings of the ieee conference on computer vision and pattern recognition, 2013, pp. 2531–2538.
- [26] Rui Shi, Wei Zeng, Zhengyu Su, Jian Jiang, Hanna Damasio, Zhonglin Lu, Yalin Wang, Shing-Tung Yau, and Xianfeng Gu, *Hyperbolic harmonic mapping for surface registration*, IEEE transactions on pattern analysis and machine intelligence (2016).
- [27] Rui Shi, Wei Zeng, Zhengyu Su, Yalin Wang, Hanna Damasio, Zhonglin Lu, Shing-Tung Yau, and Xianfeng Gu, *Hyperbolic brain surface registration with curvature-based landmark matching*, International conference on information processing in medical imaging (ipmi), 2013, pp. 159–170.
- [28] Lujin Wang, Xianfeng Gu, Klaus Mueller, and Shing-Tung Yau, *Uniform texture synthesis and texture mapping using global parameterization*, The Visual Computer **21** (2005), no. 8-10, 801–810.
- [29] Yalin Wang, Wei Dai, Yi-Yu Chou, Xianfeng Gu, Tony F Chan, Arthur W Toga, and Paul M Thompson, *Studying brain morphometry using conformal equivalence class*, 2009 ieee 12th international conference on computer vision, 2009, pp. 2365–2372.
- [30] Yalin Wang, Wei Dai, Xianfeng Gu, Tony F Chan, Shing-Tung Yau, Arthur W Toga, and Paul M Thompson, *Teichmüller shape space theory and its application to brain morphometry*, International conference on medical image computing and computer-assisted intervention, 2009, pp. 133–140.
- [31] Yalin Wang, Xianfeng Gu, Tony F Chan, Paul M Thompson, and Shing-Tung Yau, *Brain surface conformal parameterization with the slit mapping*, 2008 5th ieee international symposium on biomedical imaging: From nano to macro, 2008, pp. 448–451.
- [32] ———, *Conformal slit mapping and its applications to brain surface parameterization*, International conference on medical image computing and computer-assisted intervention, 2008, pp. 585–593.
- [33] Yalin Wang, Xianfeng Gu, Kiralee M Hayashi, Tony F Chan, Paul M Thompson, and Shing-Tung Yau, *Brain surface conformal parameterization*, Computer graphics and imaging, 2005, pp. 76–81.
- [34] Yalin Wang, Lok Ming Lui, Xianfeng Gu, Kiralee M Hayashi, Tony F Chan, Arthur W Toga, Paul M Thompson, and Shing-Tung Yau, *Brain surface conformal parameterization using riemann surface structure*, IEEE transactions on medical imaging **26** (2007), no. 6, 853–865.
- [35] Tsz Wai Wong and Hong-kai Zhao, *Computation of quasi-conformal surface maps using discrete beltrami flow*, SIAM Journal on Imaging Sciences **7** (2014), no. 4, 2675–2699.
- [36] Xiaotian Yin, Junfei Dai, Shing-Tung Yau, and Xianfeng Gu, *Slit map: conformal parameterization for multiply connected surfaces*, International conference on geometric modeling and processing, 2008, pp. 410–422.
- [37] Xiaotian Yin, Yinghua Li, Wei Han, Feng Luo, Xianfeng David Gu, and Shing-Tung Yau, *Computing shortest words via shortest loops on hyperbolic surfaces*, Computer-Aided Design **43** (2011), no. 11, 1449–1456.
- [38] Wei Zeng, Lok Ming Lui, Xianfeng Gu, Shing-Tung Yau, et al., *Shape analysis by conformal modules*, Methods and Applications of Analysis **15** (2008), no. 4, 539–556.

- [39] Wei Zeng, Rui Shi, Yalin Wang, Shing-Tung Yau, Xianfeng Gu, Alzheimer Disease Neuroimaging Initiative, et al., *Teichmüller shape descriptor and its application to alzheimer disease study*, International journal of computer vision **105** (2013), no. 2, 155–170.
- [40] Min Zhang, Ren Guo, Wei Zeng, Feng Luo, Shing-Tung Yau, and Xianfeng Gu, *The unified discrete surface ricci flow*, Graphical Models **76** (2014), no. 5, 321–339.